

An undergraduate study of harmonic and parametric motion of a simple spring-mass system from motion waveforms

I. Boscolo, F. Castelli, and M. Stellato*

Dipartimento di Fisica, Università degli Studi di Milano and

Istituto Nazionale di Fisica Nucleare—Sezione di Milano, via Celoria 16, 20133, Italy

(Dated: November 27, 2024)

Abstract

The spring-mass system studied in undergraduate physics laboratories may show complex dynamics due to the simultaneous action of gravitational, elastic, and torsional forces, in addition to air friction. In this paper, we describe a laboratory exercise that caters to beginning students while giving those with more background an opportunity to explore more complex aspects of the motion. If students are not given predefined apparatus but are allowed to design the experiment setup, they may also learn something about physics thinking and experimental procedure. Using results thus produced, we describe a variety of spring-mass oscillation patterns, discussing the physics of the significant deviations from simple harmonic motion. The parametric oscillation behavior we have observed is reported and investigated. This study is based on analysis of motion waveforms.

I. INTRODUCTION

A mass hanging from a spring is a common, easy-to-perform experiment often used to introduce first-year physics students to simply harmonic motion.¹ Although the apparatus is simple and inexpensive, under certain conditions it turns out that the motion is not simple at all.²⁻⁸ Gravitational (pendulum), elastic (spring), and torsional forces^{2,3,5,8} generate numerous, complex phenomena that result in surprising motions in the spring-mass system. These phenomena include multimode operation (many oscillating modes can be simultaneously active),⁸ parametric instability (oscillation instabilities when the system is driven at certain frequencies), and energy transfer between the spring-bouncing mode and the pendulum-swinging mode. A real spring-mass system behaves as a simple harmonic oscillator only under specific conditions: (i) the spring's mass must be negligible compared to the attached mass; (ii) the frequency of elastic oscillation must not resonate with the frequency of pendular swinging; and (iii) initial spring stretch must be strictly vertical.

A spring-mass system assembled with different values for mass and for spring constant can occasionally fall into a configuration where its elastic oscillation frequency ω_k and its pendulum-oscillation frequency ω_p have a ratio of nearly two. In such cases, the motion is unstable and the mass passes from vertical to horizontal oscillation in apparently random fashion, showing parametric rather than harmonic oscillations. (A parametric oscillator is a harmonic oscillator that has a parameter oscillating in time.) In the spring-mass system, the gravitational force acting along the axis of the spring varies periodically with the pendular motion of the mass. This periodic action results in an exchange of energy and much more complex motion. The vertical oscillation amplitude decreases while the pendular amplitude increases, and vice-versa.

We noticed that an interaction between vertical and pendular oscillations sometimes occurred in our laboratory when students are free to choose the springs and masses themselves. The physical aspects of the configurations that are linked to parametric behavior required further research to understand. Thus, we performed a study of motion waveforms for a variety of frequency ratios that spanned the resonance value $\omega_k/\omega_p = 2$. The frequency ratio is selected at will according to the equation

$$\frac{\omega_k}{\omega_p} = \frac{\sqrt{k/m}}{\sqrt{g/\ell}}, \quad (1)$$

where k is the spring constant, m is the appended mass, g is the gravitational field strength, and $\ell = \ell_0 + mg/k$ is the equilibrium length of the vertical oscillating spring, ℓ_0 being the natural (unstretched) spring length.

In order to perform this experiment, students must deal with the gap between theory and practice, examine complex, multi-effect motion, and master experimental techniques. Moreover, they have to treat data statistically and purge the experiment of many “nuisances.” In other words, the students are forced to develop the ability to manage unexpected experimental observations. The complexity of a phenomenon that is not fully understood requires a strategy for singling out the motion components, relaxing their interrelations so as to treat each component separately. Afterwards, these components can be combined to understand the complete motion. In short, this experiment turns out to be a useful, guided-research activity for students.

The theoretical work starts with the idealized equation of motion for the deviation $z(t)$ from the (vertical) equilibrium position for a mass on a spring

$$\frac{d^2z(t)}{dt^2} + \frac{C}{m} \frac{dz(t)}{dt} + \frac{k}{m} z(t) = 0, \quad (2)$$

where C is a damping coefficient. The experimental goal is to test the solution

$$z(t) = z_0 e^{-\gamma t} \cos(\omega t), \quad (3)$$

where z_0 is the initial oscillation amplitude, $\gamma = C/2m$ is the damping constant, and

$$\omega^2 = \frac{k}{m} - \left(\frac{C}{2m}\right)^2 = \omega_k^2 - \gamma^2. \quad (4)$$

In these equations, the mass of the spring is assumed to be zero, which is not actually the case. The damping force is assumed to be proportional to velocity, although air friction against a moving object depends on its shape and is not (generally) linear with velocity. The investigation proceeds through the following steps: (a) test of Hooke’s law $F = -k \Delta z$, (b) test of $\omega^2 = k/m$, (c) measurement of the damping time $\tau = 1/\gamma$, and (d) test of the sinusoidal solution Eq. (3).

In the following sections, we describe the procedure followed in laboratory work with students and point out its critical steps. In the final section, we present the experimental research work we carried out in preparation for teaching the course. This study is meant to provide a deeper grounding for those conducting a widely used experiment; it is also a

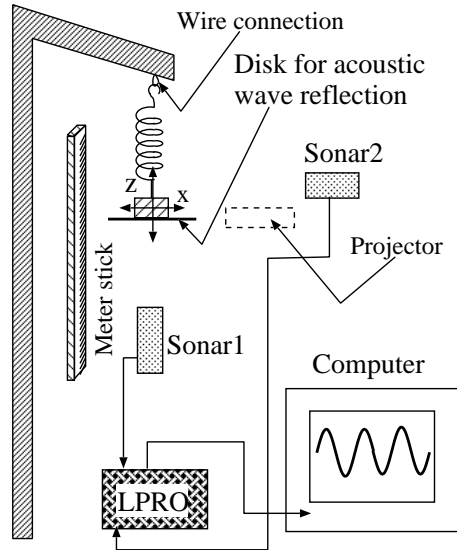


FIG. 1: Experiment layout. A meterstick and a light projector are used for measuring spring extension, while motion detectors (sonars) detect the motion. The digital data-acquisition tool LPRO (Vernier Logger Pro) acquires and sends the coordinates $z(t)$ and $x(t)$ to the computer. The top arm is bent to avoid reflecting the sonar signal.

possible topic for open-ended investigation or small, individual research projects. Complete investigation of the spring-mass system also requires studying forced oscillations,¹ which is to be the subject of further research.

II. THE SETUP

The apparatus was kept as simple as possible: just a spring and a weight oscillating vertically as shown in Fig. 1. A short piece of wire acts as a pivot. The z - and x -coordinates of the hanging mass, defined in relation to its equilibrium position, are tracked by the bottom (Sonar1) and lateral (Sonar2) ultrasonic motion detectors, respectively. The system is surrounded by plastic foam to absorb the direct sonar waves not reflected by the mass-bob. The latter is a pile of 20 g metal disks on a support, to which plasticine may be added to obtain the desired precise weight. The support is terminated by a diskette of 70-mm diameter to reflect the sound waves emitted by the bottom sonar as much as possible. This technique is necessary because the mass has wide lateral oscillations and wobbles around its pivot. Another spurious motion can be observed, namely: transverse spring vibration, possibly

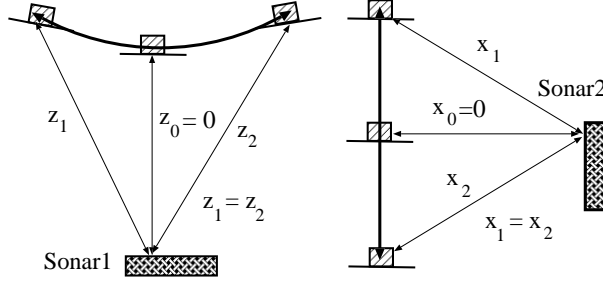


FIG. 2: Scheme of the sound-wave paths between sonars and appended masses going through transverse motions. Sonars measure the to-and-fro component of movement. Transverse motion is seen as a difference in length between the two triangle sides connected to a sonar.

due to the mass wobbling. The value of the diskette diameter is a compromise between a larger size for ideal sonar detection and a smaller size in order to minimize both friction and spurious motion. These haphazard motions, superimposed on the bouncing and pendular oscillations, cause observed motion waveforms to be irregular. Distorted waveforms prevent us from attempting a simple analysis of the experiment and of its physics content. To minimize spurious motion, it is essential to start with smooth, precise initial mass displacement and to use small oscillation amplitudes.

The two sonars ought to measure vertical and transverse oscillation exclusively, but this is not always the case. Sonar1, which is used to detect vertical oscillation, partially detects transverse, pendular oscillation as well, as sketched in Fig. 2. Similarly, Sonar2, meant to detect the transverse motion, also detects vertical spring oscillation. This leads to waveforms in which an oscillation with smaller amplitude is superimposed on the main oscillation. The resulting distortion of the oscillation under study can be observed by restricting the oscillations to pure motions. For pendulum motion, the spring was replaced with a wire; for vertical motion, a thin metal stick was inserted along the spring axis. The observation of pure motions is useful as a basis to interpret the results of combined oscillations described in the following sections.

It is worth mentioning that vertical motion detection by Sonar1 is not affected by the rotation of the pendular oscillation plane, but this is not true with Sonar2. When the oscillation plane rotates by large angles, Sonar2 waveforms become almost useless. Good waveforms from Sonar1 are enough to study the motion, with the occasional help of some information from Sonar2.

A meterstick and a stopwatch are used to measure elongations and oscillation periods, respectively. Typical values of the spring parameters are $m_{\text{spring}} \simeq 4.8 \text{ g}$, $k \simeq 8 \text{ N/m}$, and rest length 18 cm. The effective mass values for the bob—equal to the hanging mass plus a third of the spring’s mass^{1,4,8,11} (discussed more fully below)—range from 40–80 g.

In class, students assemble the system using the bottom Sonar1 only. This paper consists mainly of research performed after the students had completed the lab, and was carried out to investigate their unexpected results.

III. TEST OF HOOKE’S LAW AND $\omega^2 = k/m$

In our simple harmonic motion experiment, students determine the spring constant in the traditional way. A test of Hooke’s law $F = -k \Delta z$ is performed by adding different masses to the spring and measuring the relative static elongations using a meterstick. The spring constant is obtained with a precision of a few percent. The test of $\omega^2 = k/m$ is performed using masses ranging from a maximum value, limited by spring damage, to a minimum value, determined by excessive vibrations. Some oscillations turn out to be very irregular, particularly when smaller masses are used. Hence, students are guided towards using a larger mass to obtain more regular oscillations. The oscillation period is measured using a stopwatch. The initial objective was to verify $\omega^2 = k/m$, rewritten in terms of the period T as

$$m = \frac{k}{4\pi^2} T^2. \quad (5)$$

A graph of the added mass versus T^2 shows the expected straight line with a small negative intercept on the y -axis, as shown in Fig. 3. This test shows the effect of the non-negligible mass of the spring. A class discussion of the situation¹ leads to the conclusion that the spring’s mass cannot be neglected, and that the added mass should be replaced by an effective mass that can be written $m_e = m + m_s$, where m_s is the effective contribution of the spring’s mass. Hence, Eq. (5) must be rewritten as

$$m = \frac{k}{4\pi^2} T^2 - m_s. \quad (6)$$

The y -intercept from the data then gives the expected value of one-third of the total spring mass ($m_s = m_{\text{spring}}/3$), as reported in the literature.^{4,11} For the remainder of this paper,

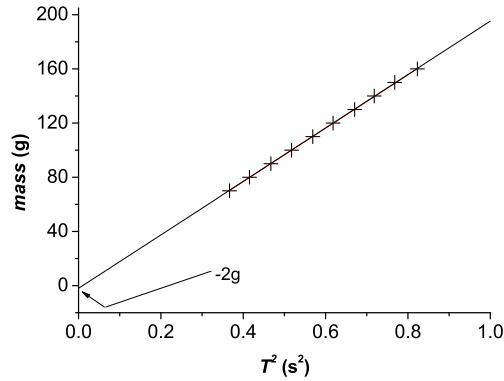


FIG. 3: Graph of Eq. (6), showing the negative intercept at the y axis.

the pendulum mass will actually refer to the effective mass as defined here unless stated otherwise.

While students notice that lighter masses cause more complex oscillations, they also realize that the system does not show the expected simple harmonic oscillation and ask assistants for help. The new phenomenon of parametric oscillations comes to the fore for the first time in this context, and the complexity of the movement leads to further measurements with multiple motion detectors connected to a computer.

IV. DECAY TIME AND FREQUENCY MEASUREMENTS USING MOTION WAVEFORMS

After completing the previous tests, students start taking measurements for the decay time $\tau = 1/\gamma$ in Eq. (3). The time interval between the beginning of the oscillation and the moment when the amplitude is reduced to $1/e$ of its initial value is measured using a stopwatch. Students use larger masses to get reasonably stable oscillations. They observe that τ depends on initial oscillation amplitude and on the value of the added mass (as expected from the definition $\tau = 2m/C$).

At this point, the study of the motion using waveforms is introduced, with the aim of measuring the two parameters τ and ω directly from the computer screen to check their previously obtained results. In theory, the value of decay time is constant for a given mass; nevertheless, we measure it for different sections of the same decay curve obtaining different values. Indeed, the decay does not appear to be exponential towards the end of the

curve, instead showing decay times that increase with time. The very slow decay at the tail indicates an effective reduction of the damping coefficient; that is, a reduction of the effect of air resistance when the mass oscillates more slowly. As a result, the mathematical form of Eq. (3), based on a constant decay value, does not reproduce actual, observed motion. Initial fast decay indicates the possibility of energy transfer from the vertical motion to other motions. For the sake of thoroughness, we add that the assumed linear dependence of the damping time τ on the hanging mass ($\tau = 2m/C$) was tested, with better than 80 percent agreement.¹

After recording the variation in decay time along the waveform curves on the screen, students use the same graphs to measure oscillation frequency. They determine the time interval relative to a set of oscillations on the computer screen, then use a fast Fourier transform (FFT) tool, part of their data acquisition software, which provides the frequency spectrum. In this context, students are introduced to the concept and use of the FFT tool. After this measurement, students take a look at the waveforms obtained with different masses. The seemingly harmonic behavior with heavy masses, the very complex motion with elastic vertical and transverse pendular oscillation interchange, and the strong variation of waveform decay at the beginning of the motion make it clear that a new and more complete model for the system is needed to account for the many discrepancies between the simple motion predicted by the theory of harmonic oscillation and actual experimental observations at variance with expected results.

Separately, a few highly-motivated students then further studied the discrepancy between theory and experiment by fitting the experimental waveform to the function $f(t) = a(0) \exp(-t/\tau) \sin(\omega_0 t + \phi) + b$. The values of $a(0)$, τ , and ω_0 (initial amplitude, decay time, and oscillation frequency, respectively) are extracted from the waveform as explained above. Fitting the whole waveform turned out to be impossible; reasonably good fits were obtained only within sections of the decaying waveform. The farther the waveform section the longer the relative τ .

As an example, the fit of a mathematical model to a waveform using a 70 g mass gives the following results, which are in accord with the previous conclusion: (1) $\tau \sim 12$ s for the first 10 s section, (2) $\tau \sim 17$ s for the first 20 s (a longer section averages two different measured decay times), (3) $\tau \sim 20$ s for the curve section $\Delta t = 10$ –30 s, (4) $\tau \sim 30$ s for the curve section $\Delta t = 20$ –60 s, and (5) a much longer result at the curve tail. We checked the

perfect correlation between the τ enhancement at a curve section and the relative frequency enhancement at that curve section, as expected theoretically from Eq. (4).

V. MEASUREMENTS ON HARMONIC AND PARAMETRIC MOTIONS

The remainder of this paper describes details of faculty members' research on motion coupling within the spring-mass system. This analysis is beyond the level of first-year undergraduate teaching. Typical waveforms obtained with a set of 70 g, 60 g, 50 g, and 40 g masses are shown in Fig. 4.

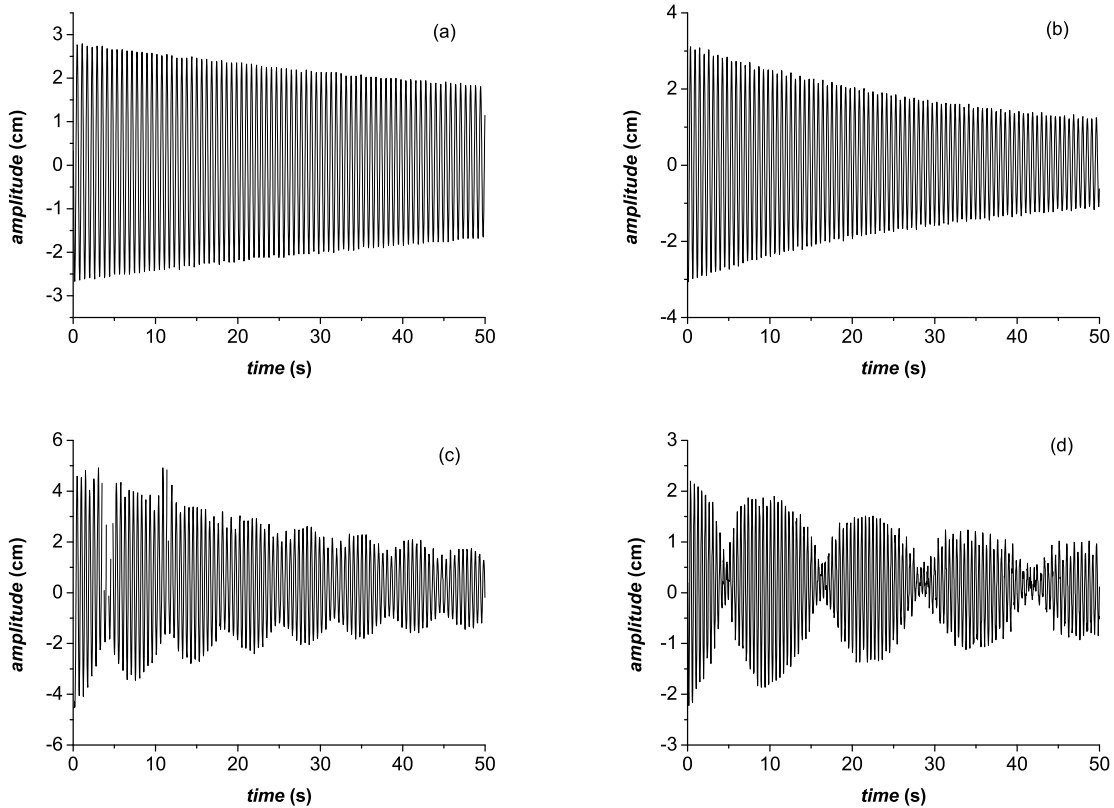


FIG. 4: Waveforms (a), (b), (c), and (d) corresponding to 70 g, 60 g, 50 g, and 40 g masses, respectively. The system passes from out-of-resonance, with the 70 g mass and $\omega_k/\omega_p \simeq 1.67$, to near-resonance, with the 40 g mass and $\omega_k/\omega_p \simeq 2.04$. The waveforms evolve from a classical, damped sine wave towards complete modulation. The comb-like crests along the signal envelope, evident in frame (d), are generated by the particular way Sonar1 detects the transverse motion component.

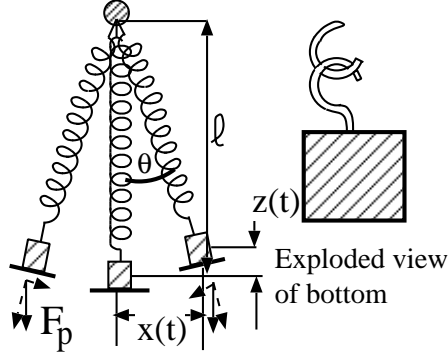


FIG. 5: Sketch of the applied force showing coupling between spring-bouncing and pendulum-swinging motions. The mass' center of gravity is not along the spring axis.

Waveforms from heavier to lighter masses show a transition from an exponential decaying sinewave to partially modulated decaying sinewaves and, finally, to a multi-lobed, completely modulated sinewave. The same developments are observed when looking directly at the motion, with composite vertical-pendular motion for masses of intermediate value and the addition of frequent switches between vertical and pendular oscillations with the lightest mass. The intermediate case of a modulated-edge sinewave indicates that oscillation exchange between the two modes is partial. By counting the lobes, we can measure the frequency of oscillation-mode exchange. Another interesting observation is that the plane of pendular oscillation is not stable. It rotates by a few degrees in the case of low partial mode exchange. Conversely, when mode exchange is complete, the oscillation plane shifts by larger angles (up to 90 degrees) in an apparently random manner.

The study of waveforms leads us to conclude that there are two different classes of motion: harmonic and non-harmonic. The two types of motions refer to different physical phenomena.

Let us again look at the forces acting in the system, as depicted in Fig. 5. We note that the component along the spring axis of the force mg applied by the appended mass changes periodically during pendular oscillation and, in turn, alters spring extension. In particular, stretching-force oscillation causes the spring's equilibrium length to oscillate around its initial value ℓ :

$$\ell(t) = \ell + \delta\ell(t). \quad (7)$$

Therefore, pendular and spring-oscillation modes are coupled. Spring extension due to the

weight makes a complete oscillation in half the time of one complete pendulum oscillation at resonance, that is when the ratio between the two oscillation periods T_k and T_p is $1/2$.

The coupling between pendular oscillation and spring oscillation induces parametric instability between the two modes^{2,3,9,10} when the resonance condition is met. The energy exchange between the modes, tested by the waveform envelope modulation, is observed up to a frequency ratio [Eq. (1)] of about 1.8. The farther from the resonance condition, the lower the energy exchange. The observed mode exchange within an interval of frequency ratio reproduces the common physical fact that the resonance curves have Gaussian-like form with a certain width. We can say that our resonance has a relatively large width. Moreover, out of resonance, our measurements show that the greater the amplitude of vertical oscillation, the more extensive mode exchange becomes, yielding a wider resonance curve. The resonance curve was also observed to enlarge as motion disorder increases, i.e. when spurious motion becomes significant compared with the two motions of spring oscillation and pendulum oscillation. Spurious motion is always present when oscillations are large. Both spurious motion and large oscillation lead to an increase of the mode coupling.

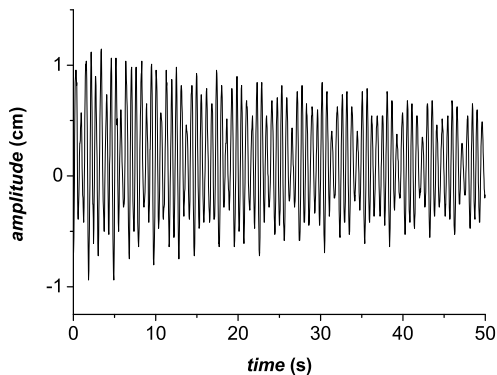


FIG. 6: Waveform of vertical oscillation obtained after a lateral initial displacement. The irregular shape of the waveform depends on the simultaneous presence of vertical and transverse oscillations, as seen by Sonar1. A 70 g mass was used in this test.

Motion due to oscillatory mode exchange (parametric motion) is initiated by either vertical or lateral shift of the appended mass, i.e. with either elastic or pendular oscillation excitation. Vertical motion represented by a waveform like that of Fig. 6 is generated by starting pendular oscillation with lateral displacement of the appended mass. This paramet-

ric motion suggests that the coupling between pendular and elastic oscillations is nonlinear. In the literature, equations describing nonlinear coupled pendulum and spring oscillations are given as²

$$\frac{d^2x(t)}{dt^2} + \omega_p^2 x(t) = c x(t) z(t), \quad (8)$$

$$\frac{d^2z(t)}{dt^2} + \omega_k^2 z(t) = c \frac{x^2(t)}{2}, \quad (9)$$

where the coupling constant c is a function of the system parameters.² Incidentally, damping is not considered in these equations. More refined motion equations that satisfactorily describe the results of our experiment are presented in Ref. 3. These equations can be obtained through Lagrangian formulation. This system can be solved analytically only in one particular case² and numerically in all others.³

The presence in the motion of different oscillation modes can be observed directly in the waveform spectrum lines obtained with the FFT tool. The spectra of the waveforms in Fig. 4, shown in Fig. 7, have the expected frequency lines for the oscillations those waveforms represent. The neater the waveform (i.e. the more ordered the motion), the neater the FFT. In each frame, the line corresponding to ω_k is largely dominant, and the line corresponding to ω_p is present, albeit with limited intensity. In disordered motion, the lines for spurious oscillation modes show up in the spectra. The two (c) and (d) spectra of Fig. 7 make the $2\omega_p$ harmonic stand out, because the pendular oscillation has large amplitude and Sonar1 doubles the pendular frequency, as explained in Fig. 2.

A. Behavior with mixed vertical and transverse excitation

Any excitation (initial mass shift with vertical and lateral components) that corresponds to a frequency ratio within the resonance width can start mixed vertical and pendular motion. Indeed, the coupling term on the right-hand side of motion equations (8) and (9) shows that an initial $x(0) \neq 0$ causes the onset of energy exchange between the two modes. It is almost impossible to apply a pure vertical or a pure lateral shift by hand.

The result obtained with mixed excitation is interesting: energy bouncing between the two modes occurs even with relatively heavy masses, i.e. with a frequency ratio that is out of resonance. The waveform obtained with 80 g mass (1.63 frequency ratio) proves to be

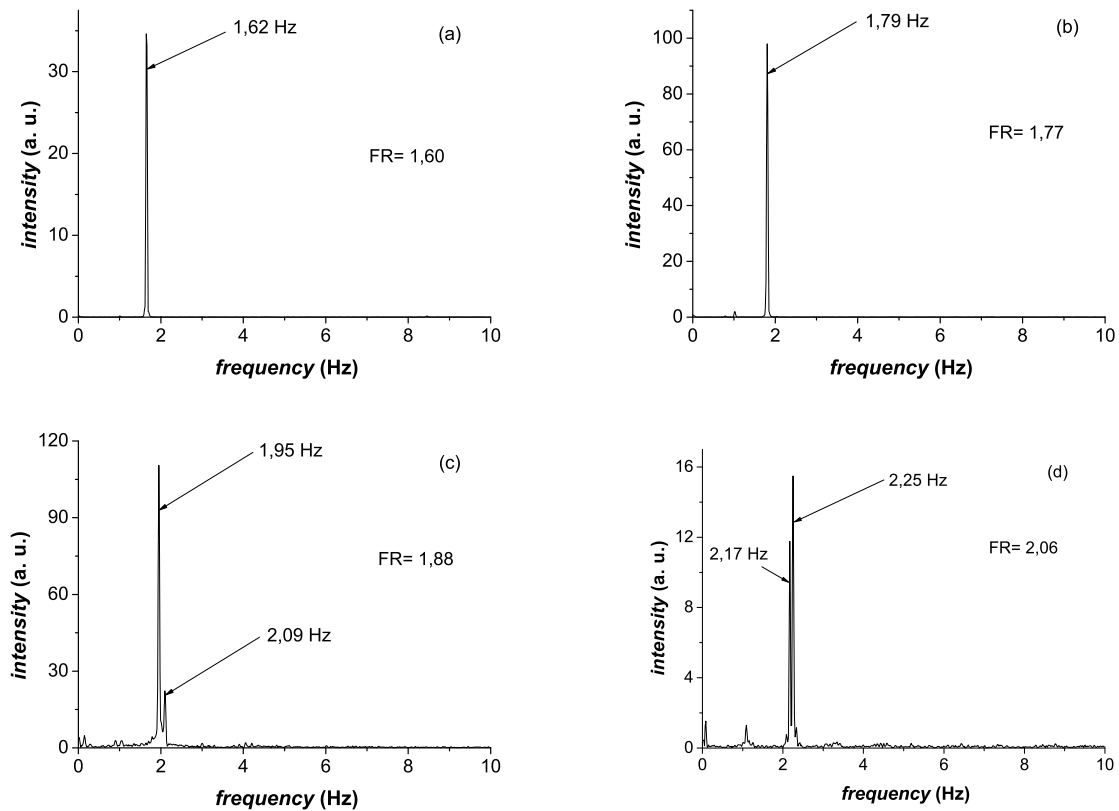


FIG. 7: Plots (a), (b), (c), and (d) show the FFT signals derived from 70 g, 60 g, 50 g, and 40 g waveforms, respectively. FR is the actual value of the frequency ratio. The frequencies of some pronounced spectrum lines are labeled.

modulated as shown in the first frame of Fig. 8. Its FFT spectrum has many sharp lines, as shown in the second frame of Fig. 8. A rather intriguing observation is that the system set itself in the peculiar stable motion shown in Fig. 9 after a few oscillation cycles—a behavior cited also in Ref 2. Results of mixed-excitation experiments enable us to state that nonlinear coupling between the two modes occurs even far from resonance.

Other observations worth reporting are:

- (1) At resonance, both vertical and lateral mass displacements lead to similar system instability.
- (2) Near resonance conditions, both strong vertical and strong lateral mass displacements lead to substantially similar results in waveforms and spectra. This is not the case with small displacements: a small vertical displacement excites only vertical spring os-

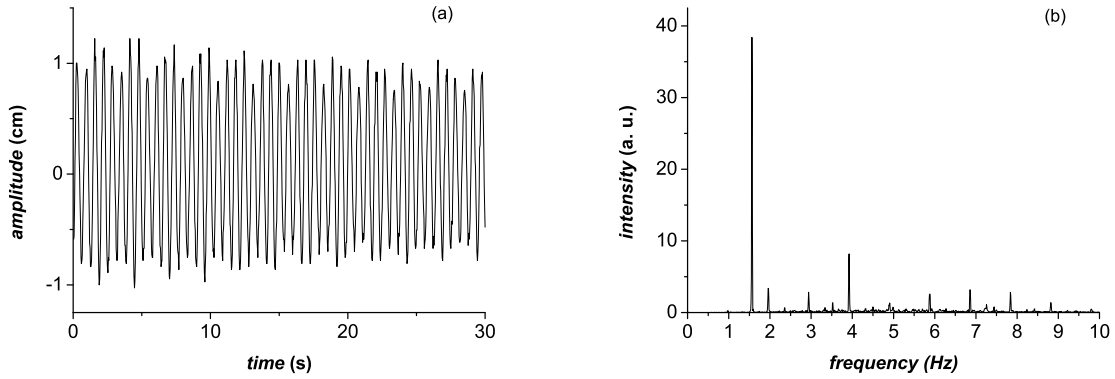


FIG. 8: Frame (a): Waveform obtained with an 80 g mass and small diagonal displacement. The energy exchange between the two modes is clearly visible. Frame (b): Frequency spectrum. Many lines are present, besides the spring frequency at 1.55 Hz and the pendular frequency at 0.95 Hz (with very small amplitude). Second harmonic frequencies are visible. Other clear lines, at higher frequencies, correspond to wobble motions.

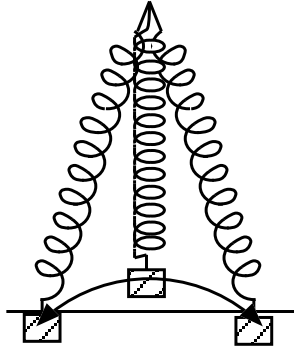


FIG. 9: Motion figure normally assumed by masses above 60 g.

cillation (no exchange with pendular oscillation), whereas a small lateral displacement excites both modes.

- (3) Mixed excitation produces complete energy transfer between the two modes even at the frequency ratio $\omega_k/\omega_p = 1.8$. The spectra are neater than in pure vertical excitation.

B. Analogy to optics

Parametric instability is common in nonlinear optics. This phenomenon is employed extensively to produce and amplify laser waves at diverse desired frequencies.^{12,13} A pump wave ω_1 launched across a nonlinear crystal generates, from noise, a signal wave ω_2 along with a so-called idler wave ω_i . Among others, the main condition that must be satisfied is

$$\omega_1 = \omega_2 + \omega_i. \quad (10)$$

In our spring-mass system, the spectrum clearly shows the idler frequency,

$$\omega_i = \omega_k - \omega_p. \quad (11)$$

For example, the spectrum of the waveform yielded by vertically exciting a 70 g mass shows the idler line distinctly, as seen in Fig. 10. This figure reproduces a selected section of the spectrum recorded by Sonar2, which, for this type of excitation, detects low-amplitude components more cleanly.

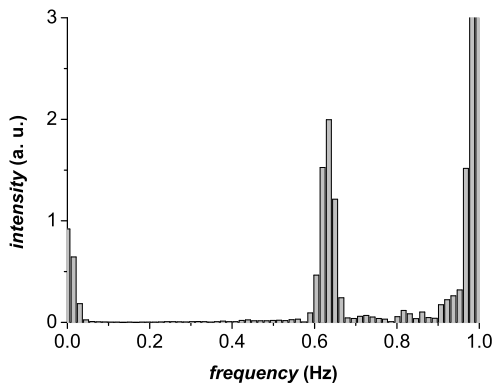


FIG. 10: The idler frequency line at $0.62 = (1.63 - 1.01)$ Hz from the FFT graph of the waveform generated by vertically exciting a 70 g mass (see Fig. 7(a)), recorded by Sonar2.

VI. CONCLUSION

The vertically oscillating spring-mass system used to study harmonic oscillator physics in a first-year laboratory course has to be pre-designed in order to reliably reproduce the motion described in textbooks. In a laboratory organized so that students can assemble their

own apparatus as they see fit (picking components from a pile), the spring-mass system is not likely to turn out so that it reproduces the idealized harmonic motion. There is a good chance they will come up with a system that shows complex dynamics. Furthermore, to test the spring-mass physics law $\omega^2 = k/m$, students have to apply different masses, thus often running into parametric instability. Hence, studying the spring-mass system in a laboratory where students pick the parts addresses both harmonic and parametric behavior. We believe the spring-mass experiment can be treated in class as a harmonic oscillator and then developed towards the parametric oscillator. This teaching sequence allows students to approach the challenging, complex physics content of parametric behavior.

One of this paper's main contributions is its experimental investigation of the parametric motion of the spring-mass system, as dealt with in the first-year laboratory course for physicists. The study was performed by tracking the motion of the appended mass with an ultrasonic motion detector and capturing the waveform on a computer screen. Analysis of the waveform clearly reveals the parametric instability and the energy exchange between the bouncing spring and the swinging, pendular oscillation, when the resonance conditions between the two oscillations are met. Resonance width is measured by looking at waveforms in a frequency interval around the resonance.

The rather complex—but manageable—experiment and the gap between the ideal theoretical case and the actual experimental case make this experiment a useful tool for stimulating an aspiring physicist's thinking. We are working on a presentation of a more in-depth study of parametric spring-mass physics.

Acknowledgments

We thank M. Giliberti for useful hints, and R. Lowenstein for supporting this research and for critical reading of the manuscript. We gratefully acknowledge technical assistance from D. Cipriani.

* Electronic address: marco.stellato@unimi.it

¹ I. Boscolo and R. Loewenstein, "The spring-mass experiment as a step from oscillations to waves: mass and friction issues and their approaches," *Lat. Am. J. Phys. Educ.* **5**, 409–417

- (2011).
- ² M. G. Olsson, “Why does a mass on a spring sometimes misbehave?,” *Am. J. Phys.* **44**, 1211–1212 (1976).
 - ³ T. E. Cayton, “The laboratory spring-mass oscillator: an example of parametric instability,” *Am. J. Phys.* **45**, 723–732 (1977).
 - ⁴ J. Christensen, “An improved calculation of the mass for the resonant spring pendulum,” *Am. J. Phys.* **72**, 818–828 (2004).
 - ⁵ R. Geballe, “Statics and dynamics of a helical spring,” *Am. J. Phys.* **26**, 287–290 (1958).
 - ⁶ E. E. Galloni and M. Kohen, “Influence of the mass of the spring on its static and dynamic effects,” *Am. J. Phys.* **47**, 1076–1078 (1979).
 - ⁷ H. L. Armstrong “The oscillating spring and weight—an experiment often misinterpreted,” *Am. J. Phys.* **37**, 447–449 (1969).
 - ⁸ J. T. Cushing, “The spring-mass system revisited,” *Am. J. Phys.* **52**, 925–932 (1984).
 - ⁹ H. M. Lai, “On the recurrence of a resonant spring pendulum,” *Am. J. Phys.* **52**, 219–223 (1984).
 - ¹⁰ D. E. Holzwarth and J. Malone, “Pendulum period versus hanging-spring period,” *Phys. Teach.* **38**, 47 (2000).
 - ¹¹ D. Halliday, R. Resnick, and K. S. Krane *Physics, Vol. 1*, 4th ed. (John Wiley & Sons, New York, 1992), p. 336, problem n.25.
 - ¹² A. Yariv, *Quantum Electronics*, 3rd ed. (John Wiley & Sons, New York, 1988), p. 411.
 - ¹³ S. Cialdi *et al.*, “Efficient two-step Positronium laser excitation to Rydberg levels,” *Nucl. Instr. Meth. Phys. Res. B* **269**, 1527–1533 (2011).